

1 We thank both reviewers and Henrike Wilms for their many helpful comments, most of which
2 we have incorporated in the new version of our manuscript (found below with changes in blue).
3 In the time since the first submission of this manuscript the OSIRIS data was updated. We have
4 also implemented the suggestion of Henrike Wilms of starting nucleation also at later times,
5 and in order for all simulations to be of the same length, we have restricted the simulation time
6 to 24 hours. This gave us a more varied data set and has resulted in some smaller changes in
7 the results, as can be seen in some of the figures, but the main messages remain. For instance,
8 the occurrence rate in figure 8 has changed somewhat. The reason that, since it takes some time
9 for the clouds to develop, the occurrence rate is somewhat sensitive to the arbitrary chosen start
10 and end time of the simulation, and thus changed as we use 24 h instead of 48 h simulation
11 time. Nevertheless, the occurrence frequency for the Wave Clouds remain in better agreement
12 with OSIRIS than the No Wave clouds. We have updated the text to comply with these changes.
13 We have also changed the y-scale in figure 7 from logarithmic to linear in order to make it more
14 clear how insensitive the particle retrieval is to the smaller sizes.

15

16

17 Reply to reviewer 1 (The comments of the reviewer are in *italic*):

18

19

20 *General Comments*

21 *1) The paper investigates the inherent errors in retrieved PMC particle size,*
22 *concentration, and mass density, when using remote observations. This addressed by*
23 *using modeled PMC properties to simulate the OSIRIS signals, and then conducting*
24 *retrievals of size, concentration, and mass density from these signals. Comparisons of the*
25 *known and retrieved PMC properties give a solid indication of the errors / biases inherent to*
26 *the observations and the chosen methodology. The conclusions of this paper are important for*
27 *remote sensing of PMCs. The model based studies indicate that OSIRIS retrievals have greater*
28 *errors for smaller particle sizes.*

29 *2) The second aspect of the paper is to determine if inclusion of atmospheric waves in*

1 *PMC microphysical models gives a better reproduction observed PMC properties,*
2 *compared to using a static atmosphere. The Author's find that simulations with waves*
3 *indeed give the best explanation of observed PMC properties, as shown in Figures 6 and 7. The*
4 *conclusions here are important for PMC modeling efforts, however, the*
5 *representation of waviness in the model (section 4.2) is somewhat brief. Is it possible to describe*
6 *the wave parameters used in more detail, perhaps in such a way that other*
7 *modelers could implement a scheme like yours? Also, the agreement in Fig 7 between the*
8 *OSIRIS and wavy model is not spot on. Is it possible that some wave tuning would give better*
9 *agreement (and thus indicate a refined picture of the relevant waves)?*

10
11

12 In response to this comment and the one from Henrike Wilms we have added a figure with the
13 temperature and wind fields used so that other modellers can compare to their work, or use
14 similar fields if they wish.

15

16 The idea of tuning the model to give a better representation of the waves is indeed interesting.
17 The current data set is too small to allow for this but it may be possible with the upcoming
18 MATS satellite which will use tomographic retrieval to get 3D information of temperature and
19 PMC and where a much larger data set will be available. We have added a discussion of this
20 idea to the manuscript.

21
22

23 *Specific Comments*

24 *Throughout: "modelled" should be "modeled".*

25 According to the windows spelling checker "modelled" is UK English and "modeled" US
26 English. Since ACP is a European journal we assume UK spelling should be used and thus
27 leave this as it is.

28 *Throughout: In PMC / NLC literature "IWC" usually refers to the vertically integrated water*
29 *content (g / km²). You assign IWC units of ng/m³, which would be ice mass density (m). You*

1 *need to change IWC for m_i (or M_i) throughout. (I know IWC is a clumsy and probably misplaced*
2 *acronym, but it is widely recognized as g / km^2 in the PMC field).*

3 This has been changed according to the suggestion.

4 *p 1 line 12: I don't think we capitalize Noctilucent, or Polar Mesospheric Cloud.*

5 This has been changed according to the suggestion.

6 *p 1 line 13: add "ground based remote sensing" to the list*

7 This has been changed according to the suggestion.

8 *p 1 line 19: "...on signals based on modeled..."*

9 This has been added according to the suggestion.

10 *p 2 line 10: This statement is missing something, you state that PMCs are a means to*
11 *monitor the atmosphere, but do not state which aspects of the atmosphere.*

12 This has been changed to "...a way to monitor changes in this remote region of the
13 atmosphere..."

14 *p 2 line 25: "number density" typically refers to the number of gas molecules per cc. If you are*
15 *referring to ice particles, then typical nomenclature would be "ice concentration (N)".*

16 This has been changed according to the suggestion.

17 *p 3 lines 4-7: The comment in parenthesis can just be a sentence.*

18 This has been changed according to the suggestion.

19 *p 3 line 12: Again, to be precise, you retrieve PMC properties from signals simulated*
20 *using modeled size distributions.*

21 This has been changed according to the suggestion.

22 *p 4 line 18: "...spectral resolution of..."*

23 This has been changed according to the suggestion.

24 *p 4 line 25: I think this should be "...fixed at 16 nm for radii larger than 40 nm...". You should*
25 *also state that many other remote sensing PMC experiments have adopted this assumption, e.g.*
26 *CIPS, SOFIE, SCHIAMACHY, SBUV, & probably others.*

27 This has been changed according to the suggestion.

1 p 4 line 27: Is there a reference that supports the choice of $AR = 2$?

2 Reference added.

3 p 4 lines 27-30: You are describing the two-valued solutions for certain conditions. This could
4 be stated more clearly.

5 This has been changed according to the suggestion.

6 p 5 line 15: It would be useful to state the SMR vertical and horizontal resolution.

7 This has been added.

8 p 6 line 13: Here you should cite the recent study by Killani et al (ACP 2015) that deals with
9 non-spherical ice in microphysical PMC models. The main point is that there are microphysical
10 effects due to non-spherical shapes that change the modeled PMC properties, in addition to the
11 well known optical effects of non-spherical ice.

12 This has been added according to the suggestion.

13 p 6 line 29: You should also mention that ice sublimation enhances vapor at the ice layer
14 bottom. Does SMR detect the dry and wet regions associated with ice?

15 This has been mentioned. Yes, the SMR data show several regions of enhanced water vapour
16 concentration at the altitudes corresponding to the lower layer of NLCs. However, as the water
17 vapour enhancement created by a cloud can linger far after a cloud has sublimated, a direct
18 correlation between cloud presence and enhancement is not seen in the dataset.

19 p 7 line 25: "(fraction of 1 nm)" should be stated as "(radii < ~1 nm)"

20 This has been changed according to the suggestion.

21 Figure 1: You should add the frost point temperature vs. height, this would make your
22 arguments on p 7 flow very easily. Also, it would be instructive to add error bars as the standard
23 deviations to give an idea of the natural variability. "OSISIS" - "OSIRIS"

24 The standard deviation of the OSIRIS temperature is shown in figure 5. Here we choose to only
25 present input to the stationary model.

26 p 8, lines 17-18 & 32 (and elsewhere): You often mix units and nomenclature for ice
27 mass. For example "ice water density" is stated as being in ng/m^3 , where I would
28 consider these units to be associated with "ice mass density". Later you refer to "ice

1 *mass" which I assume is "ice mass density". Perhaps introduce a variable "m sub i" if*
2 *that would make the discussion more convenient, in any case make the language*
3 *consistent.*
4 We now use "ice mass density" or " m_i " throughout the manuscript.
5 *p 9 line 1: What specifically is the OSIRIS IWC observation mentioned here? Is it the*
6 *average associated with the SMR data in Figure 1, or something else?*
7 This has been clarified.
8 *p 9 line 25: By "constant" do you mean "constant in height" ?*
9 We do not find the wording "constant" at the indicated place but we have clarified what we
10 mean by "constant" in 4.2.
11 *p 10 line 11: "less than" should be "broader than"*
12 There appears to be something wrong with the page and line indications. We assume the
13 reviewer means the vertical resolution of OSIRIS and has changed that according to the
14 suggestion.
15 *p 10 line 13: Do you really pass the model size distributions through the OSIRIS retrieval*
16 *algorithm? I would think that you use the model distributions to simulate OSIRIS signals, and*
17 *then pass these signals through the retrieval code. Please clarify.*
18 This has been reformulated.
19 *p 10 line 19: I think you mean that the microphysical treatment of ice particles in*
20 *CARMA assumes spheres. But when you do the OSIRIS signal simulations, do you*
21 *assume spheres or AR=2? This aspect of the signal simulation should be stated. Again, Killani*
22 *et al. [2015] discuss the microphysical implications AND the optical retrieval implications for*
23 *non-spherical NLC particles, and that work is relevant to your study and thus should be*
24 *mentioned.*
25 Yes, that is what we meant, this had been clarified and the work of Kiliani et al. is mentioned.
26 *p 10 line 28: Please clarify what "mean radius" refers to (e.g., numeric mean, mass*
27 *weighted mean, the Gaussian median, ...).*

1 This has been added to the figure caption.

2 *p 10 line 28: Panel b of which figure?3*

3 Yes, this has been corrected.

4

5 *p 11 line 7-9: Part of the challenge is that the error in concentration (N) is proportional to the*
6 *cube of the radii error. The propagation of radii errors into the other values exists because you*
7 *determine radii first, and then mass density and N (presumably based on the modeled signal*
8 *based on retrieved radii). In any case, you should discuss further the reasons for N having the*
9 *greatest errors.*

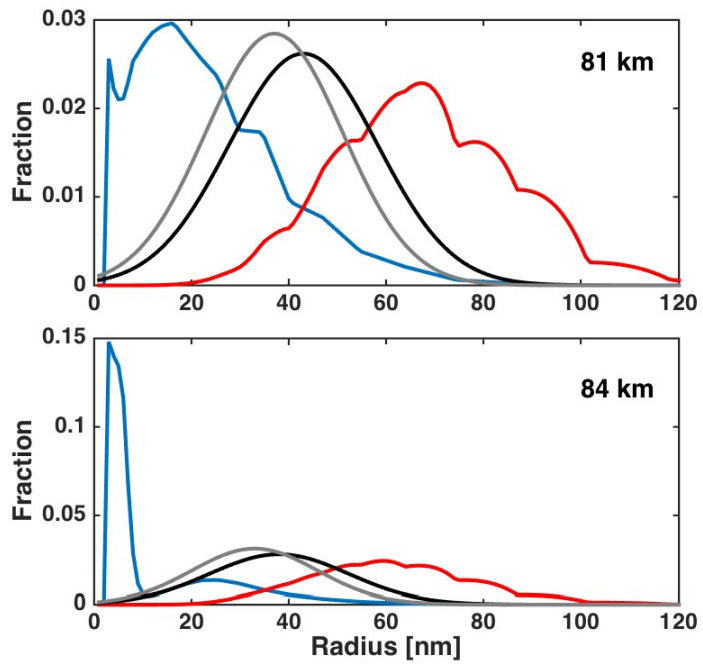
10 This has been added.

11 *p 11 line 20: The retrieval cannot be based on Mie scattering since you accommodate*
12 *non-spherical particles. Indeed, you state above that the optical calculations are from the T-*
13 *matrix algorithm.*

14 This has been reformulated.

15 *p 11 lines 21-22: There may be a better explanation for why the retrieval indicates larger*
16 *particles than the numeric mean. I suspect the reason is that the smallest particles do not*
17 *contribute to the OSIRIS signal. I think this would be evident if you plot the fraction of total*
18 *radiance in each size bin of the size distribution. If this explains the discrepancy (I think it will),*
19 *then showing the additional figure would be very useful (I don't think anyone has published this*
20 *and it could settle some old debates).*

21 Yes, this is exactly what we mean with that OSIRIS is more sensitive to larger particles – so
22 that smallest particles will not contribute to the signal. This is the reason we do not see the
23 many small particles. But if we have a multimodal distribution with one mode at a very small
24 particle size then the effect is that we miss that mode completely and thus make a large error in
25 the estimate of total ice particle concentration. We have changed the text so that this becomes
26 clearer and we have changed the y-scale of figure 7 so that it becomes even more obvious how
27 much of the particles we are insensitive too. We liked the idea of such a plot and made it (see
28 below, note that the y-axis differs slightly from the one in the paper) but we found that it is
29 confusing for the reader. Therefore, we simply shaded the region where 90% of the signal
30 comes from in the paper instead.



1

2 *p 12 lines 18-28, and Figure 6: You switch between "rate" and "frequency", the later*
 3 *would be convention.*

4 This has been changed.

5 *Figure 7: This might be clearer if you showed standard deviations instead of all the*
 6 *individual profiles (thin lines).*

7 We have changed this plot in line with the suggestion apart from that we use percentiles since
 8 the distributions are non-normal.

9 *p 13 line 20: The statement "...exist when the temperature is below the average,..." is*
 10 *unclear. The average is of what group of data?*

11 This has been reformulated.

1 *p 13 lines 21-25: The no wave case (thick black) is zero below 82 km, so the statement*
2 *does not make sense. Perhaps you meant the wave case. You should remind us to look at Figure*
3 *7c.*

4 Yes, we meant the wave case. Thank you.

5 *p 13 lines 28-32: Some of this is hard to see because of the many thin lines in the plots. I do,*
6 *however, see your basic points here, and you should not that both the ALOMAR lidar and*
7 *SOFIE have shown this behavior as well, where N peaks at an altitude above the peak in ice*
8 *mass density, and radii are largest below the peak in mass density.*

9 This has been removed. It still seems to be the case if you look at individual profiles but if you
10 look at the mean, median or percentiles it is not the case. (These properties becomes different
11 from individual profiles because at altitudes that clouds are the most frequent they are the
12 calculated from many profiles but as we go to altitudes where the clouds rarer there are less
13 profiles left from which these properties are calculated and those that are left are those of the
14 brighter clouds.) So we have chosen to remove this part.

15 *p 16 line 7: I believe the correct name is "PMC microphysics and happy hour working group".*

16 Indeed. We thank the reviewer, who clearly is an expert in the field, but keep the current
17 wording in order to not confuse more the general public (smile).

18

19

20 Reply to reviewer 2:

21

22 We agree that we should point out more clearly that we can reproduce the results of Rapp and
23 Thomas and have done so in the updated manuscript. We have also added a figure with the
24 temperature and wind fields used as input for the model.

25

26 Reply to Henrike Wilms:

27 We have added a figure showing the temperature and wind fields used as input for our model.

28 We have also now started the nucleation process at not only 0 h, 10 h, and 20h do get more
29 variations in the clouds.

1
2
3
4
5
6
7

9

1
2
3
4
5
6
7
8
9
10
11
12
13
14
15
16
17
18
19
20
21
22
23
24
25
26
27
28
29

Comparison of retrieved [noctilucent](#) cloud particle properties from Odin tomography scans and model simulations

Deleted: Noctilucent

[Linda Megner](#)¹, [Ole M. Christensen](#)¹, [Bodil Karlsson](#)¹, [Susanne Benze](#)¹, and [Victor I. Fomichev](#)²

- Deleted: L.
- Deleted: O.
- Deleted: B.
- Deleted: S.
- Formatted: Superscript
- Deleted: V.

[1]{Department of Meteorology, Stockholm University, Sweden}
[2]{CRESS, York University, Canada}

Correspondence to: L. Megner (linda@misu.su.se)

Abstract

Formatted: English (US)

Mesospheric ice particles, known as [noctilucent](#) clouds or [polar mesospheric clouds](#), have long been observed by rocket instruments, [satellites](#) and [ground based remote sensing](#), while models have been used to simulate ice particle growth and cloud properties. However, the fact that different measurement techniques are sensitive to different parts of the ice particle distribution makes it difficult to compare retrieved parameters such as ice particle radius or [ice concentration](#) from different experiments. In this work we investigate the accuracy of satellite retrieval based on scattered light and how this affects derived cloud properties. We [apply](#) the retrieval algorithm on [spectral signals calculated from](#) modelled cloud distributions and compare the results to the properties of the original distributions. We find that ice mass density is accurately retrieved whereas mean radius often is overestimated and high [ice concentrations](#) generally are underestimated. The reason is [a combination of that measurements based on scattered light are insensitive to the smaller particles and](#) that the retrieval algorithm assumes a Gaussian size distribution, whereas the modelled size distributions often are multimodal. Once we know the limits of the satellite retrieval we proceed to compare the properties retrieved from the modelled cloud distributions to those observed by the Optical, Spectroscopic, and Infrared Remote Imaging System (OSIRIS) instrument on the Odin satellite. We find that a model with

- Deleted: Noctilucent
- Deleted: Polar Mesospheric Clouds
- Deleted: and
- Deleted: particle number density
- Deleted: run
- Deleted: number densities
- Deleted: ,
- Deleted: ,

1 a stationary atmosphere, as given by average atmospheric conditions, does not yield cloud
2 properties that are in agreement with the observations, whereas a model with realistic
3 temperature and vertical wind variations does. This indicates that average atmospheric
4 conditions are insufficient to understand the process of [noctilucent](#) cloud growth and that a
5 realistic atmospheric variability is crucial for cloud formation and growth. Further, the
6 agreement between results from the model - when set up with a realistically variable atmosphere
7 - and the observations suggests that our understanding of the growth process itself is reasonable.

Deleted: Noctilucent

8

9 1 Introduction

10 At the summer polar mesopause, the coldest region on Earth, the temperature drops low enough
11 so that ice particles can form despite the low water content of a few parts per million. These ice
12 clouds, known as [noctilucent](#) clouds (NLCs) or [polar mesospheric clouds](#) (PMCs), provide a
13 way to monitor [changes in](#) this remote region of the atmosphere, where in situ measurements
14 can only be carried out using rockets. NLCs have been observed by the naked eye since the late
15 19th century (Leslie, 1885) and since the second half of the 20th century, rocket instruments,
16 satellites, lidars and models have been used to develop our understanding of the clouds (e.g.
17 Witt, 1960;Turco et al., 1982;Barth et al., 1983;Hansen et al., 1989).

Deleted: Noctilucent

Deleted: Polar Mesospheric Clouds

18 The different measurement techniques used in remote sensing and for in situ measurements -
19 and even by particular types of instruments within these categories - make it difficult to compare
20 retrieved parameters such as ice particle radius or [ice concentration](#) from different experiments.

Deleted: particle number density

21 For example, many in situ rocket measurements are not sensitive to the size of the particles, as
22 long as they are above a certain aero-dynamical threshold that is determined by the shape of the
23 instrument and the speed of the rocket (Hedin et al., 2007). Remote sensing instruments like
24 satellites and lidars on the other hand, are more sensitive to the particles that more efficiently
25 scatter or absorb light, i.e. the particles at the larger end of the size distribution. They, in
26 particular the instruments that observe scattered light, are thus rather insensitive to the smaller
27 end of the size distribution. A direct comparison of for example the [ice concentrations](#) measured
28 by in situ and remote sensing techniques is therefore not straight forward.

Deleted: number densities

29 Even comparisons between individual satellite observations have proven very difficult (Bailey
30 et al., 2015). These difficulties are also due to the fact that different measurement techniques
31 inevitably favour different parts of the size distribution. For instance, an instrument that
32 measures the absorption of light will be sensitive to the total volume of the ice while an

1 instrument that observes scattered light will be sensitive to different regions of the size
2 distributions depending on what scattering angles it observes. If, as earlier studies have
3 indicated, the size distribution were truly Gaussian with a certain width (see e.g. Rapp and
4 Thomas, 2006), then this problem would be easier to overcome, but as will be shown in this
5 study, our model simulations suggest that this is not generally the case.

6 The size distribution of ice particles in the cloud layer varies with altitude, Models predict that
7 they range from hundreds or thousands freshly nucleated small particles per cubic centimetre
8 at the mesopause to ten or less more mature particles per cubic centimetre at approximately 81-
9 83 km (Megner, 2011). This means that the question of which part of the size distribution an
10 instrument is sensitive to is intricately connected to which altitude region the instrument is
11 sensitive to.

12 In this paper we therefore first investigate the accuracy of the Odin satellite's retrieval of
13 properties such as ice mass density (m_i), mean radius, and total ice concentration. We do this
14 by applying the retrieval algorithm on spectral signals calculated from modelled cloud
15 distributions (which obviously are fully known) and comparing the retrieved results to the
16 properties of the original distributions. After this we proceed to compare the properties retrieved
17 from the modelled cloud distributions to those observed by satellite. We use satellite
18 observations from the Odin tomography modes (Hultgren et al., 2013) for which the satellite's
19 scanning sequence is specifically designed to provide multiple measurements through the same
20 cloud volume, which enables, via tomography, high resolution altitude and horizontal
21 observations of the NLCs. We use information from both instruments on-board the Odin
22 satellite: the Optical Spectrograph and InfraRed Imager System (OSIRIS) instrument
23 (Llewellyn et al., 2004) gives us high resolution data of the NLCs and the Sub-Millimeter
24 Radiometer (SMR) instrument (Nordh et al., 2003) provides information of the background
25 temperature and water vapour, which in this experiment are used as input to our model.

26 The specific aims of this study are to:

27 1) Identify what part of the size distribution we capture with an OSIRIS-type measurement and
28 to evaluate to what extent retrieved properties - such as mean radius, m_i and ice particle
29 concentration - of the sampled volume represent corresponding actual properties.

30 2) Investigate if our current knowledge of the microphysics (as represented by the CARMA-
31 model) is accurate enough to simulate clouds that match our observations, and to pinpoint what
32 model input is crucial for simulating representative clouds.

Deleted: (models

Deleted: ;

Deleted: water content (IWC

Deleted: number density.

Deleted: running

Deleted: IWC

Deleted: number density

1 The paper is structured as follows: In section 2 the Odin tomography scans and the retrieval
2 algorithms of OSIRIS and SMR are described. In section 3 the microphysical model is
3 described. Section 4 gives the results of the comparisons and finally section 5 summarizes the
4 conclusions.

5

6 **2 Odin tomography scans**

7 Both OSIRIS and SMR observe the atmosphere in the limb geometry: the co-aligned optical
8 axes of both instruments sweep over a selected altitude range in the forward direction as the
9 entire satellite is nodded up and down. During the stratosphere/mesospheric mode, both
10 instruments scan from 7 to 107 km. However, during the tomography mode, only the NLC
11 region of interest, 78 to 90 km, is scanned. This decreases the horizontal distance between
12 subsequent scans and increases the number of lines of sight through a given atmospheric
13 volume, thus enabling the tomographic retrieval of cloud and background atmosphere
14 properties. During the NH10 and NH11 seasons, a total of 180 orbits were performed using the
15 tomographic mode. The orbits were chosen to provide coincident observations with the
16 Aeronomy of Ice in the Mesosphere (AIM) satellite and cover three three-day periods during
17 each NLC season (Table 1, Hultgren et al., 2013). A tomographic retrieval algorithm is then
18 used to convert the limb-integrated atmospheric line-of-sight properties into local information
19 about cloud properties or the background atmosphere (Christensen et al., 2015;Hultgren and
20 Gumbel, 2014;Hultgren et al., 2013). Using the tomographic algorithm these local properties
21 can be retrieved between 78 and 87 km with a horizontal and vertical resolution of ~330 km
22 and 1 km, respectively. For this analysis we use four days of tomographic data (76 scans)
23 between 70° N and 77° N of July 2010 and 2011, where SMR and OSIRIS data both are
24 available. During these days, clouds and background atmosphere were sampled at Solar
25 Scattering Angles of 70° to 100°.

26

27 **2.1 OSIRIS retrieval**

28 The tomographic algorithm transforms the observed OSIRIS limb radiances into the retrieved
29 volume scatter coefficient, a measure of cloud brightness. In contrast to the input limb radiance,
30 which is dependent on tangent altitude and thus contains signals from fore- and background,
31 the retrieved volume scatter coefficient is a local signal dependent on the vertical dimension

Deleted: °

1 altitude and the horizontal dimension Angle Along Orbit (AAO). The algorithm used is the
2 Multiplicative Algebraic Reconstruction Technique (MART) based on maximum probability
3 techniques (Hultgren et al., 2013; 2014).

4 OSIRIS observes scattered sunlight at wavelengths between 277 and 810 nm, with a [spectral](#)
5 resolution of approximately 1 nm. For this study, the volume scatter coefficient at specific
6 wavelengths in the UV-range (277.3 nm, 283.5 nm, 287.8 nm, 291.2 nm, 294.4 nm, 300.2 nm,
7 and 304.3 nm; see e.g. Karlsson and Gumbel, 2005, for details) is used to retrieve particle sizes
8 from the OSIRIS radiance measurements by fitting the observed spectral signal to tabulated
9 scattering spectra from numerical T-matrix simulations (Baumgarten and Fiedler, 2008;
10 Mishchenko and Travis, 1998). Once a particle mode radius is retrieved, [ice concentration](#), and
11 ice mass density can be estimated. [In accordance with many other satellite retrieval algorithms](#)
12 [\(e.g. CIPS, SOFIE, SCHIAMACHY, SBUV\)](#), a Gaussian particle size distribution with a width
13 that varies as 0.39 times the retrieved mean radius but stays fixed at [16 nm](#) for [radii larger than](#)
14 [40 nm](#) (Baumgarten et al., 2010), [is assumed](#). Further, the particles are assumed to be oblate
15 spheroids with an axial ratio of 2, [\(Eremenko et al., 2005\)](#).

16 The retrieval size for mode radius is constrained to < 100 nm. This is because [there is more than](#)
17 [one solution when fitting the observed signal to the simulated T-matrix spectra for large](#)
18 [particles and scattering angles >90 degrees \(see von Savigny et al., 2005, their figure 3, for an](#)
19 [equivalent issue\)](#). [The lack of a unique solution makes it impossible](#) to distinguish between
20 particles > 100 and smaller particles (around 50 nm) in the approach we are using. A
21 consequence of this constraint is that the algorithm will select a small mode radius that fits the
22 signal even in the presence of really large particles. Whether this is an acceptable shortcoming
23 in the retrieval algorithm or not is out of the scope of this study; our conclusions are not affected
24 by this constraint.

25
26 The PMC microphysical retrieval and resulting uncertainties in cloud brightness and
27 microphysical products are described in detail by Hultgren et al. (2013) and Hultgren and
28 Gumbel (2014). Based on uncertainty in the input radiances, they estimate a typical statistical
29 error in cloud brightness of $10^{-11} \text{ m}^{-1} \text{ str}^{-1}$, which is less than 1% of the typical NLC peak
30 brightness. Propagating the error of the individual radiances through the tomographic retrieval
31 algorithm, statistical uncertainties in mode radius ($\sim \pm 6 \text{ nm}$ throughout all altitudes), [ice](#)
32 [concentration](#) (from $\pm 1 \text{ cm}^{-3}$ at 81 km to $\pm 35 \text{ cm}^{-3}$ at 86 km), and ice mass density (negligible
33 at lower PMC altitudes, up to $\pm 5 \text{ ng m}^{-3}$ at 86 km) are estimated.

Deleted: number density

Deleted: The

Deleted: assumes

Deleted: ,

Deleted: 15.8

Deleted: radii

Deleted: .

Deleted: .

Formatted: Justified

Deleted: is not possible

Deleted: (see e.g. von Savigny and Borrows, 2007, for an equivalent issue).

Deleted: number density

1 2.2 SMR retrieval

2 SMR measures thermal emission from the 557 GHz water vapour line. From this, the
3 concentration of water vapour and temperature can be retrieved in the aforementioned altitude
4 region. This can be achieved as the line is very strong and becomes optically thick even in the
5 MLT region. The retrieval is done using the non-linear optimal estimation method with a
6 Levenberg-Marquardt iteration scheme. The resulting precision is 0.2 ppmv for water vapour
7 mixing ratio and 2 K for temperature, [with a vertical resolution of 2.5 km and a horizontal](#)
8 [resolution of 200 km](#). The data used in this study are all collected when SMR was operating in
9 frequency mode 13, as this mode shows the best agreement with other satellite instruments
10 (within 5 K for temperature and 20% for water vapour). For further details see Christensen et
11 al. (2015).

12 3 CARMA model

13 Community Aerosol and Radiation Model for Atmospheres (CARMA) is a microphysical cloud
14 model that originated from a stratospheric aerosol code
15 (Toon et al., 1979;Turco et al., 1979) that was developed to simulate clouds in a variety of
16 environments ranging from the Earth's atmosphere to other planetary atmospheres. It has been
17 used to simulate NLCs in numerous publications (e.g. Asmus et al., [2015](#); [Kiliani et al.](#),
18 [2015](#); Chandran et al., 2012; Megner, 2011; Megner et al., 2006; Rapp and Thomas, 2006; Merkel
19 et al., 2009; Stevens, 2005; Vergados and Shepherd, 2009; Lübken et al., 2007). As in the
20 majority of these studies, we use the 1-dimensional setup of the model to simulate
21 microphysical processes such as ice nucleation and growth, sedimentation and vertical
22 transport. Three interactive constituents are simulated: Condensation Nuclei (CN), ice particles
23 and water vapour. The CN are assumed to be meteoric smoke particles with a density of 2
24 g/cm³. The number density and size distribution of the CN are representative of the middle of
25 the NLC season (July 10th) at 68°N (see Figure 1 in Megner et al. (2008a)). The nucleation is
26 treated in the framework of droplet theory (Fletcher, 1958) where the probability of nucleation
27 depends on the size of the CN and the contact angle. The contact angle, also known as the
28 wettability, in turn depends on the surface energies between nucleus, ice and air (Fletcher,
29 1958; Keesee, 1989; Gumbel and Megner, 2009; Megner and Gumbel, 2009). While this quantity
30 remains uncertain, it has been argued that meteoric smoke acts very efficiently as ice nuclei
31 (Roddy, 1984; Rapp and Thomas, 2006) and the contact angle is therefore set to 0.95 in
32 agreement with previous studies (Megner, 2011; Megner et al., 2008a; Rapp and Thomas, 2006).

Deleted: .

1 [Apart from the details mention above our model setup is similar to that of Rapp and Thomas](#)
2 [\(2006\): The model domain spans from 72 to 102 km in altitude with a resolution of 0.25 km.](#)
3 The ice particles are considered spherical and the size distributions are evaluated on radius grids
4 consisting of 40 non-equally spaced size bins between 2 to 900 nm. The piecewise parabolic
5 method algorithm (Colella and Woodward, 1984) is used for both vertical advection and
6 deposition growth (advection in particle radius space) with a time step of 100 s. Following Rapp
7 and Thomas (2006) we [further](#) use an eddy diffusion profile adapted from the collection of
8 turbulence measurements at 69° N under polar summer conditions (Lübken, 1997). [In](#)
9 [all model runs we allow for 5 hours for initialisation after which the next 24 hours are used in](#)
10 [the analysis.](#)

Deleted: The model domain spans from 72 to 102 km in altitude with a resolution of 0.25 km.

11

12 **4 Results**

13 As explained in Section 2, the Odin tomography scans give us simultaneous high resolution
14 observations of ice particles from OSIRIS and water vapour and temperature from SMR. We
15 use these SMR observations as input to the CARMA model and then compare the modelled
16 clouds to those observed by OSIRIS. However, we cannot use the water vapour and temperature
17 profiles from an SMR observation that is made simultaneously to the OSIRIS observation of
18 ice particle properties as initial state for the model. The reason is that ice growth is not an
19 instantaneous process, i.e. the environment that the clouds grow in is not necessarily the same
20 as the environment they are observed in. For instance the ice growth process itself uses up much
21 of the available water, [leading to depletion of water close to the mesopause where the ice grows](#)
22 [and enhancement of water where it sublimates.](#) Since we do not have any observations of the
23 history of the atmospheric environment in which the cloud developed we cannot compare a
24 single observed cloud directly to its modelled equivalent. We therefore have to settle for a more
25 statistical approach, by comparing general clouds that are observed by OSIRIS to modelled
26 clouds that have developed in the typical atmospheric environment that SMR observes. In
27 Sections 4.1 and 4.2 we investigate [different](#) ways of creating such a typical environment from
28 the SMR observations and report about the clouds they produce. As presented in the
29 introduction, one main goal of this study is to identify what part of the size distribution we
30 capture with the OSIRIS-type instrument retrieval and how this is reflected in the retrieved
31 properties such as mean radius, [ice mass density and ice concentration.](#) In Section 4.3 we
32 investigate this by [retrieving sizes from the modelled cloud distributions by applying the same](#)

Deleted: leaving a depleted water profile.

Deleted: two

Deleted: IWC and number

Deleted: of particles.

Deleted: running

Deleted: retrieval algorithm on

1 [method that we use for the OSIRIS retrievals](#) and comparing the retrieved results to the original
2 distribution. Finally, in Section 4.4 we compare the modelled clouds to those observed by
3 OSIRIS.

4 **4.1 The Stationary Atmosphere**

5 In order to generate a typical cloud growth environment from the SMR measurements we select
6 observations that are co-located with the OSIRIS tomography scans where no clouds were
7 present. By selecting only the measurements where no clouds are present we avoid the problem
8 of not accounting for water that is already in the ice phase. We then calculate the average water
9 vapour and temperature profiles and use these fields to drive the model. Since SMR data is only
10 trustworthy up to an altitude of 87 km we extended the water vapour profile linearly above this
11 altitude, while for the temperature profile we used the SABER profile from Sheese et al. (2011)
12 as shown in Figure 1. Since SMR does not measure vertical wind we follow Rapp and Thomas
13 (2006) and [use](#) a vertical wind profile representative of 69N as given by Berger (2002). The
14 temperature, water vapour and wind profiles in this run are thus stationary. In this model setup,
15 only a very minor m_i of maximum 0.03 ng/m^3 developed. This is far below the detection
16 threshold of OSIRIS of 5 ng/m^3 . Hence, if the model is driven by mean atmospheric conditions
17 as measured by the SMR instrument it will not produce visible clouds. The main reason is
18 simply that the small ([radii < ~1 nm](#)) meteoric smoke particles are not efficient condensation
19 nuclei at a temperature of approximately 131 K (the mesopause temperature shown in Figure
20 1), see Gumbel and Megner (2009). We note that the model setup used in Rapp and Thomas
21 (2006) does in fact result in observable clouds ([and our model reproduces their result given the](#)
22 [same input](#)). This is because they use the meteoric smoke distribution of Hunten et al. (1980),
23 which is based on a one-dimensional model of ablation and recombination of meteoric material
24 and as such lacks meridional atmospheric transport. More recently multi-dimensional models
25 have shown that this transport efficiently depletes the summer mesopause of meteoric material
26 resulting in much smaller meteoric smoke particles in this region than what was earlier assumed
27 (Megner et al. 2008b, Bardeen et al. 2008).

28 The SMR average temperature is declining with altitude up to 87 km, where the measurement
29 quality is diminishing. Thus, it gives no information on where exactly the mesopause is. To
30 examine if a higher (and thus colder) mesopause would trigger the model to produce clouds,
31 the temperature profile above the SMR observations was extended to lower temperatures and a
32 higher mesopause using the OSIRIS temperatures (Sheese et al., 2011) as shown by the dash-

Deleted: IWC

Deleted: fraction of

Deleted: .

1 dotted line in Figure 1. Although this resulted in a larger m_i of maximum 2 ng/m³, it is still
2 below the detection threshold of OSIRIS.

Deleted: IWC

3 In order to investigate how much colder the atmosphere needs to be for the model to produce
4 clouds, the average temperature profile was reduced in steps of 1K, and used as input to the
5 model. In order to produce clouds in CARMA of similar m_i as the average clouds observed by
6 OSIRIS, the temperature profile had to be reduced by 6 K. However the particles produced by
7 this model realization were too large (150 nm) and their ice concentrations far too small (<10
8 particles/cm³ throughout the cloud region) compared to the OSIRIS tomography scan
9 observations. Apparently, clouds from this model run were not a realistic representation of the
10 clouds we observe with Odin. We can conclude that a simple shift of the temperature profile
11 towards lower values is not enough to produce realistic NLCs.

Deleted: IWC

Deleted: number densities

12 Another possibility to facilitate cloud formation is to assume that the CNs are larger, or more
13 efficient, so that they can nucleate ice particles at a higher temperature. To test this we first
14 enhanced the contact angle to unity, i.e. perfect wettability (see Section 3). This did not have a
15 major effect on the cloud properties and resulted in a maximum ice water density of 0.4 ng/m³,
16 which is still far below the OSIRIS detection limit. However, the CN distribution is dependent
17 on many uncertain parameters (Megner et al., 2006). For instance, if there is more meteoric
18 influx into the atmosphere, if the CNs are electrically charged (Gumbel and Megner,
19 2009; Megner and Gumbel, 2009), or if there is more coagulation within the meteor trail than
20 what is generally assumed in models of meteoric coagulation and transport (Megner et al.,
21 2008b; Bardeen et al., 2008), then this could result in a CN distribution that is more efficient for
22 nucleation. Thus we pose the question: What is the number density of efficient CNs required to
23 generate clouds with an m_i that agree with the OSIRIS observations? To answer this question
24 we assumed simple mono-sized distributions of particles with radii of 2 nm, i.e. large enough
25 to be efficient CN at 131 K (Gumbel and Megner, 2009) but small enough not to rapidly
26 sediment out of the mesopause region. Note, that for simplicity we here enhance the
27 condensation nuclei efficiency by making the particle larger, but the nucleation efficiency can
28 be enhanced by other means, such as charging of the particles, with equivalent results. By
29 feeding the model mono-sized particle distributions of 10, 100, 1000 and 10000 particles/cm³
30 we determined that approximately 100 efficient CNs /cm³ was needed to produce an ice mass
31 equivalent to the OSIRIS observations. It should be noted that increasing the number of CNs
32 even more has little effect on the ice mass, as pointed out by Megner (2011); the case with

Deleted: IWC

1 10000 particles/cm³ gave approximately twice the ice mass compared to the case with 100
2 particles/cm³. Despite that a CN distribution consisting of 100 particles/cm³ of 2 nm radii is not
3 considered likely - the original CN distribution from the model by Megner (2011) falls sharply
4 with radius and has on the order of 10 particles larger than 1 nm and 10⁻⁴ particles/cm³ larger
5 than 2 nm - we nevertheless show the cloud generated in this way in Figure 2 ([top panel](#)) as an
6 example of a cloud generated in stationary conditions with a highly efficient CN distribution.
7 This cloud will be referred to as the “No Wave” cloud.

8 It is however clear that the most straight forward solution to the lack of cloud development in
9 an averaged steady state atmosphere is not that a more efficient size distribution is needed, but
10 simply that the ice particles observed in the real atmosphere are nucleated during the times
11 when the temperature is below the average. This we will investigate in the next section.

12

13 4.2 Variable atmosphere

14 The mesopause region is characterized by high wave activity (e.g. McLandress et al., 2006).
15 This means that the constant temperature profile achieved by averaging the SMR measurements
16 as describe above is not representative. In order to represent the fast temperature variations and
17 vertical winds that give rise to them, we use July temperature and vertical wind fields from July
18 69°N from the extended Canadian Middle Atmosphere model (CMAM) (Beagley et al.,
19 2010;Fomichev et al., 2002;McLandress et al., 2006) with a high temporal resolution output
20 (30 minutes). In this second setup of the CARMA model we still use the SMR retrieved mean
21 temperature profile to determine the average conditions, but impose the time resolved CMAM
22 temperature field to represent the temperature variations. In practice this is achieved by adding
23 a temperature shift ([constant in time and altitude](#)) to the CMAM data so that the average CMAM
24 temperature profile matches up with the average measured SMR profile. The resulting
25 temperature [fields are shown in Figure 3](#) and the [average temperature profile with the](#) associated
26 temperature [variation is](#) shown in [Figure 5a](#) and [b](#). As can be seen the variations from the
27 CMAM model are fairly similar to those of the SMR data set, especially given that the CMAM
28 variations include diurnal variations which are not well sampled by SMR since SMR measures
29 predominantly at two local times. The variations of the CMAM model also agree well with
30 observations of daily variations in the summer polar mesopause region (Höffner and Lübken,
31 2007). Since the vertical wind is intimately connected to the temperature via adiabatic

Deleted: ,

Deleted: constant

Deleted: profile,

Formatted: Font color: Black, German

Deleted: variations are

1 heating/cooling, we use the accompanying CMAM vertical wind field to drive our model
2 simulations (Figure 4 and Figure 5 c, d). The output from the CMAM model was fed into
3 CARMA at time steps of 30 minutes.

Deleted: Figure 3 c
Deleted: d).

4 This second model setup, which includes variations in temperature and winds, resulted in clouds
5 of ρ_i above the OSIRIS detection threshold and, as we shall see, of similar ρ_i as that measured
6 by OSIRIS. An example of a cloud produced in this way can be seen in the lower panel of
7 Figure 2. We will refer to these clouds as “Wave” clouds. As the cloud development is
8 somewhat sensitive to the temperature field at the initialisation of the model we perform three
9 simulations, the original which is initialised at 0 h in (see Figure 3 and Figure 4), one which is
10 initialised at 10 h and one that is initialised at 20 h. In all simulations we allow 5 hours for
11 initialisation after which the following 24 hours are included in the analysis.

Deleted: IWC
Deleted: IWC

Formatted: Font color: Black, German

12 4.3 Modelled cloud retrieval

13 An important step when comparing the model results to observations is to run the modelled
14 clouds through a similar retrieval process. Since the OSIRIS vertical resolution is broader than
15 that of the model (1 km as opposed to 0.25 km), the first step is to linearly average the modelled
16 size distributions over four altitude levels. After that the signal from the modelled size
17 distributions are treated in the same manner as the OSIRIS observations, as described in Section
18 2.1.

Deleted: less

Deleted: passed through
Deleted: retrieval algorithm

19 In order to investigate how well the retrieval algorithm works, which part of the ice particle size
20 distribution it is sensitive to, and how this is reflected in the retrieved properties, we compare
21 the retrieved modelled clouds to the originally modelled clouds (Figure 6). As the OSIRIS
22 clouds have been retrieved with an assumption of an axial ratio of 2, whereas the microphysical
23 treatment of ice particles in the model assumes spheres, i.e an axial ratio of 1, we show the
24 retrieved properties for both of these assumptions; axial ratio of 2 in black and axial ratio of 1
25 in grey. For the “No Wave” clouds (marked with squares) the retrieval is almost entirely
26 independent of axial ratio (indeed the majority of grey squares are hidden by the black squares),
27 whereas the retrieval of the “Wave” clouds (marked with stars) is somewhat sensitive to the
28 assumption. The reason that the “No Wave” clouds show almost no sensitivity to the axial ratio
29 may be connected to that their size distributions are more well-behaved, as we will discuss later.
30 It is also worth mentioning that the axial ratio not only changes the optical properties of the
31 particles but may also impact their microphysical growth in a way that our CARMA simulation

Deleted: modelled clouds are

Deleted: It is clear from this figure that, in general, the two different assumptions generate similar results for
Deleted: retrieved properties. Indeed, many
Deleted: markers
Deleted: markers since the two assumptions give the same results.

1 with spherical particles would not capture (Kiliani et al., 2015). Panel a shows that the m_i is
 2 retrieved rather accurately, for both the “No Wave” and the “Wave” clouds, even if the retrieved
 3 m_i frequently slightly underestimates the volume, especially at higher m_i . This is encouraging
 4 since it indicates that ice mass density is a property we can trust to within approximately 30%.
 5 Figure 6b shows that the retrieved mean radius generally is larger than the original mean radius
 6 by a factor 2 to 7 for smaller radii. The retrieval of smaller radii (< 20 nm) is worse when an
 7 axial ratio of 2 is assumed which is to be expected given that our model assumes spherical
 8 particles, but for larger particles there is no clear difference. Large radii (≥ 80 nm) are,
 9 underestimated by the retrieval algorithm. The reason is simply that the retrieval algorithm is
 10 constrained to select the smaller radii out of two possible solutions, as described in Section 2.1.
 11 In practice this prevents the retrieval from retrieving particle sizes above approximately 100
 12 nm. Figure 6c shows that high ice concentrations, which generally are associated with small
 13 radii at the upper range of the clouds, are greatly underestimated. The underestimation is worse
 14 when an incorrect axial ratio (in this case 2) is assumed but can still be as larger than a factor
 15 10 for the retrieval with the correct axis ratio of 1. For instance, ice concentrations of 1000
 16 particles/cm³ are generally retrieved as around 30 particles/cm³ when a ratio of 2 is assumed
 17 and as 70 when a ratio of 1 is assumed. It is clear that these large errors in number density arise
 18 from fact that the number density depends on the radius cubed – thus a small error in mean
 19 radius will yield a large error in number density.
 20 In order to understand the underestimation of high ice concentrations and the overestimation of
 21 small mean radii we study the size distribution. Figure 7 shows a typical example of “Wave”
 22 modelled size distributions at 81 and 84 km respectively (red line), and the retrieved size
 23 distribution using an axial ratio of 2 (black line) and 1 (grey line). Since the retrieval algorithm
 24 assumes a Gaussian distribution it obviously cannot retrieve the bimodal distributions that often
 25 appear in the model. These multi-peaked distributions arise from the fact that the cold spots
 26 produced by atmospheric waves create bursts of newly nucleated particles. These particles then
 27 grow and sediment to a region where older and larger cloud particles already exist, resulting in
 28 a bimodal size distribution. This effect is more prominent closer to the nucleation region (i.e.
 29 the mesopause), and thus the size distribution is often less Gaussian at 84 km than at 81 km.
 30 Due to the nature of light scattering the retrieval is sensitive mostly to the large end of the
 31 particle distribution. This can be seen by the shaded area in Figure 7, which indicates the
 32 particles that contribute the most to the total radiance, and thus are most important for the

- Deleted: IWC
- Deleted: (marked with squares)
- Deleted: (marked with stars),
- Deleted: IWC
- Deleted: .
- Deleted: IWC
- Deleted: 20
- Deleted: Panel
- Deleted: up to about
- Deleted: 3
- Deleted: whereas
- Deleted: of around 50
- Deleted: 70 nm are well retrieved. The large
- Deleted: on the other hand (
- Deleted: and above
- Deleted: greatly
- Deleted: We note that these large radii are mostly produced in the “No Wave” clouds, which, as we shall see in Section 4.4, do not appear to be an adequate representation of the real clouds. Figure 4
- Deleted: small number densities
- Deleted: fairly large
- Deleted: lower
- Deleted: typically are overestimated, whereas higher number densities
- Deleted: (up to a factor 30 for number densities of 1000 particles/cm³)
- Deleted: large as
- Deleted: number densities

- Deleted: more
- Deleted: multi-peaked
- Deleted: Since
- Deleted: based on Mie scattering, it is

1 [retrieval \(the shaded area contributes with 90% of the total radiance\)](#). It is clear that the radiance
2 [is dominated by the contribution from the large particles and thus the retrieval will attempt to](#)
3 [fit a Gaussian to the larger side of the size distribution](#). This means that the retrieved mean
4 radius will be larger than the mean radius of the original size distribution, which explains what
5 we saw in the middle and bottom panel of Figure 6: For smaller radii (generally higher in the
6 cloud) the retrieval often overestimates the mean radius, whereas for larger radii around 50 to
7 70 nm, the agreement is better. Furthermore, the total [ice concentrations](#) are generally in good
8 agreement when [ice concentrations](#) are low (typically lower in the cloud where the size
9 distribution is less bimodal) whereas they are greatly underestimated when [ice concentrations](#)
10 are high (typically higher in the cloud, where the particles in the smaller mode are missed by
11 the retrieval).

Deleted: the larger mode or

Deleted: number densities

Deleted: number densities

Deleted: number densities

12 The “No Wave” clouds, which are simulated in a stationary environment lacking the cold spots
13 that create the bursts of fresh ice particles, generally do not show this behaviour and thus their
14 size distributions tend to be more Gaussian (see for instance Rapp and Thomas, 2006). In other
15 words, a stationary atmosphere typically tends to generate Gaussian size distributions whereas
16 temperature variations in the atmosphere generate multi-peaked, [or less Gaussian](#) particle size
17 distributions. This is the reason why the properties of the stationary clouds (squares in Figure
18 6) in general are better retrieved and their radii/[ice concentrations](#) are not
19 overestimated/underestimated in the same way as for clouds generated in a non-stationary
20 atmosphere.

Deleted: number densities

Deleted: It is worth noting that the discussed retrieval issues due to multi-peak distributions are independent of axial ratio.

22 4.4 Comparison to OSIRIS

23 We now move on to comparing the raw and retrieved modelled clouds to the OSIRIS
24 observations. In this section we only show results where an axial ratio of 2 has been assumed
25 in the retrieval, but the figures look similar and the conclusions remain the same if an axis ratio
26 of unity is used.

27

28 As mentioned earlier the OSIRIS detection threshold as expressed in m_i is approximately 5
29 ng/m^3 . In the following we will therefore select only the modelled cloud pixels where the
30 retrieved ice mass density is higher than this. However, first we investigate how often this is
31 the case, i.e. the occurrence frequency of clouds above the detection limit. [If](#) the model has an

Deleted: IWC

Deleted: After all, if

1 accurate description of the atmospheric state then the occurrence frequency in the model should
 2 be similar to that of the OSIRIS observations. However, we stress that the occurrence frequency
 3 of the model is somewhat dependent on the length of the simulation and the time allowed for
 4 initialisation of the model, so that an exact agreement cannot be expected. Figure 8 shows the
 5 altitude dependent occurrence frequency for the OSIRIS observations (in green), the retrieved
 6 “Wave” clouds (in green) and the retrieved “No Wave” clouds (in blue). While the occurrence
 7 frequency of “Wave” clouds is about twice that of the OSIRIS observations (maximising at 40%
 8 and 20% respectively), the altitudinal distributions of the clouds are similar. The “No Wave”
 9 clouds on the other hand show even higher occurrence frequency maximising at 80% and the
 10 altitude extent of the clouds is sharply cut off at 81-82 km.

11
 12 Figure 9 compares the retrieved properties of the clouds for the “Wave” clouds (in red), the “No
 13 Wave” clouds (in blue) and the OSIRIS clouds (in green). The thick lines represent the median
 14 of all profiles and the shaded fields represent the area between the 10 and 90 percentiles (we
 15 choose to plot these instead of the standard deviation since the properties are non-normally
 16 distributed). We also plot the median of the raw cloud properties (dashed lines) of the model
 17 clouds to show how they differ from the retrieved properties. Panel a shows the retrieved radius,
 18 panel b the ice concentration and panel c m_i . When comparing these properties of the clouds,
 19 it is important to remember that the “No Wave” clouds were tuned to produce the correct m_i by
 20 selecting an appropriate CN distribution, i.e. the black lines of panel c have been tuned so that
 21 their maximum magnitude corresponds to that of the green lines. One should recall that without
 22 this tuning the maximum m_i that developed was only 0.03 ng/m³, i.e. it would not be visible in
 23 the figure. The “Wave” clouds on the other hand have not been tuned to match the OSIRIS
 24 results. Despite the lack of tuning, there is a general agreement between the “Wave” clouds and
 25 the OSIRIS observations, for all the three properties; radius, ice concentration, and m_i , even if
 26 the latter is overestimated by the model at lower altitudes. This may be explained by a difference
 27 in temperature variability (Figure 5b), which results in that the occurrence of cold temperatures
 28 (<150 K) diminishes faster with altitude for OSIRIS than for CMAM (it goes below 50% at
 29 83.7 km for OSIRIS and at 81.8 km for CMAM).
 30 However, at high altitudes, the raw clouds had much higher ice concentrations and much
 31 smaller radii than what was retrieved. For example, at 86 km, the median ice concentration of
 32 the raw clouds was 273 particles/cm³ and the median raw radius was 12 nm, but the retrieval

- Deleted:** rate
- Deleted:** blue
- Deleted:** black). The
- Deleted:** rate
- Deleted:** and
- Deleted:** both maximise slightly above 20%,
- Deleted:** even if
- Deleted:** model suggests that
- Deleted:** on average appear 0.5-1 km higher than the observations, the agreement is still very good.
- Deleted:** different characteristics: the
- Deleted:** rate maximise
- Deleted:** profiles of
- Deleted:** blue
- Deleted:** black
- Deleted:** One modelled profile represents a snapshot of the modelled clouds whereas one OSIRIS profile represents a retrieved OSIRIS profile.
- Deleted:** fat
- Deleted:** mean
- Deleted:** modelled profiles or
- Deleted:** mean
- Deleted:** all OSIRIS profiles.
- Deleted:** number density
- Deleted:** the IWC
- Deleted:** IWC
- Deleted:** IWC
- Deleted:** good
- Deleted:** number density, and IWC.

1 [shows 28 particles/cm³ of 63 nm radius. The retrieval becomes marginally better for an assumed](#)
2 [axis ratio of 2 \(58 particles/cm³ of 40 nm radius, not shown\), but the basic problem remains.](#)
3 [The reasons for these under-/overestimations were discussed in the previous section. Here we](#)
4 [mainly stress that the retrieved “Wave” clouds may agree with OSIRIS observations, but the](#)
5 [measured radius and number densities cloud be far from those of the real clouds.](#)

6 Clearly the “No Wave” clouds are restricted to a [narrower](#) altitude range than the OSIRIS
7 observations and the “Wave” clouds (the altitudinal range of the “No Wave” clouds is
8 insensitive to the choice of CN distribution and thus not affected by the aforementioned tuning).
9 This is easily explained by the static temperature profile, which simply causes conditions that
10 are too warm for clouds to [grow](#) below approximately 82.5 km ([see](#) Figure 1). In the variable
11 atmosphere on the other hand the clouds can still exist [even](#) when the [average temperature \(i.e.](#)
12 [the temperature used in the static case\) is above the frost point](#), which explains the broader
13 altitudinal extent of the “Wave” clouds and the OSIRIS observations. [Again we see that the](#)
14 [retrieval algorithm works better](#) for the “No Wave” clouds, which [as earlier explained, is due](#)
15 [to their more Gaussian size distributions.](#)

16 [To summarize the “Wave” clouds agree reasonably well with the observations, whereas the](#)
17 [clouds from a stationary models are far too weak, and even if they are tuned to the correct \$m_i\$,](#)
18 [they appear in a narrower altitude region than the OSIRIS observations show. The differences](#)
19 [between the “Wave” clouds and the observations may be due to the fact that, despite our efforts](#)
20 [to create a representative background environment, the corrected CMAM temperature and wind](#)
21 [fields are not exact representations of the real background atmosphere in which the clouds have](#)
22 [been growing. Unfortunately, due to measurement errors of SMR temperature and water vapour](#)
23 [and the lack of vertical wind measurements at the mesopause, the true atmosphere is not exactly](#)
24 [known. It may be possible to tune these fields, within the uncertainty of the measurements, to](#)
25 [get an even better agreement between the modelled clouds and the observations. However, since](#)
26 [these fields are functions of altitude and time \(and obviously in the real atmosphere also of](#)
27 [horizontal position\), there are many free parameters and the limited knowledge of the](#)
28 [condensation nuclei adds even more. Therefore, such a tuning would need a significantly larger](#)
29 [data set.](#)

30

Deleted: more narrow

Deleted: exist

Deleted: the temperature reaches 150 K at 82.2 km).

Deleted: is below

Deleted: average

Deleted: One may note

Deleted: below 82 km the average IWC is higher

Deleted: than the OSIRIS clouds

Deleted: can be

Deleted: by a difference in temperature variability; the occurrence of cold temperatures (<150 K) diminishes faster with altitude for OSIRIS than for CMAM (it goes below 50% at 83.3 km for OSIRIS and at 81.8 km for CMAM).

Deleted: Another aspect where there is better agreement between the OSIRIS observations and the “Wave” clouds as compared to the “No Wave” clouds is where in the cloud layer the different quantities peak. For the OSIRIS observations and the “Wave” clouds the number density generally increases with altitude peaking above the IWC, whereas the mean radii increases with decreasing altitude and peaks at the bottom of the clouds, i.e. lower than the maximum IWC. For the “No Wave” clouds the individual profiles for mean radii, number density and IWC tend to peak at the same altitude (in Figure 7a we can see that some of the individual profiles show smaller mean radii at 83 km than at 82 km but these are the data points that were subject to retrieval issues as discussed in Section 4.3 and showed by the squares below the line in Figure 4b). -

[1]

1 **5 Conclusions**

2 In this paper we have used modelled NLC size distributions to investigate the accuracy of the
3 OSIRIS satellite retrieval algorithm by applying it on our modelled distributions and comparing
4 the retrieved properties to those of the original distributions. We show that ice mass density is
5 well retrieved (within 30 %) whereas mean radius and ice concentrations are much less
6 accurate. The retrieved mean radius is often larger than the actual mean radius especially for
7 small radii where there can be up to a factor of 7 difference. The reason for the inaccuracy is
8 that the retrieval algorithm assumes a Gaussian size distribution, and when faced with the
9 multimodal distributions that often occur in the modelled clouds (and thus likely in the real
10 atmosphere), it will attempt to fit a Gaussian to the larger side of the distribution and miss the
11 lower modes, giving an overestimate of the mean radius. Since the size distributions tend to be
12 more multi-peaked the closer to the nucleation region one gets, this happens more often higher
13 in the cloud where the particles are smaller. At the mesopause we can therefore expect large
14 differences in radius and ice concentration between the retrieved and true properties of the
15 clouds. The ice concentration on the other hand, is retrieved fairly well for small ice
16 concentrations (which generally occur lower in the cloud where the size distributions are more
17 Gaussian), but is underestimated by typically a factor of 10 or more for the high ice
18 concentrations (which generally occur higher in the clouds where the size distributions are more
19 multi-peaked).

20 We proceed to compare the retrieved modelled clouds to those of the OSIRIS tomography
21 retrieval runs. The temperature and water vapour fields used to drive the model were inferred
22 from the SMR measurements, which are collocated with the OSIRIS observations of ice
23 particles. We find that driving the model with stationary temperature and wind fields, as given
24 by the average of the SMR measurements, does not yield any observable clouds. In fact, for the
25 model to produce clouds of similar magnitude in ice content as what OSIRIS observes the
26 average temperature field needs to be reduced by 6 K, and even then the clouds that develop
27 are not representative for the OSIRIS observations in that they consist of very small ice
28 concentrations of too large particles. The reason why no clouds develop in the stationary
29 atmosphere is that the sub-nanometer meteoric smoke particles are too small to be efficient
30 condensation nuclei at the mesopause temperature of 131 K. We show that by increasing the
31 size of the CN, and thus making them nucleate more efficiently, it was possible to generate
32 observable clouds. However, in order to generate clouds of ice mass density comparable to the

Deleted: running

Deleted: IWC

Deleted: 20

Deleted: number densities

Deleted: 3

Deleted: This explains why

Deleted: overestimation

Deleted: mean radius is more pronounced for smaller radii.

Deleted: number density

Deleted: number densities

Deleted: number densities

Deleted: typically

Deleted: number densities

Deleted: IWC

1 OSIRIS observations, the CN need to be much larger than what we expect from models of
2 transport and coagulation of meteoric material, or their nucleation properties need to differ
3 significantly from the droplet theory that these models generally assume. Moreover, the
4 altitudinal extent of the clouds produced by the stationary model did not match observations. It
5 is worth pointing out that the stationary model setup used in Rapp and Thomas (2006) resulted
6 in observable clouds because they used the meteoric smoke distribution of Hunten et al. (1980)
7 which later have been shown to greatly overestimate the number of larger (> 1 nm radius)
8 meteoric smoke particles at the summer mesopause as compared to more advanced models
9 (Megner et al. 2008b; Bardeen et al. 2008). Our stationary model reproduces the results of Rapp
10 and Thomas (2006) if given the same CN distribution as input.

Deleted: .

Deleted: characteristics, e.g. the

Deleted: ,

Deleted: in this way

Deleted: ,

11
12 The region of the atmosphere where NLCs develop is far from stationary, as it is heavily
13 influenced by wave activity, which infers large fluctuations in the temperature and wind field,
14 making the actual temperature and winds very different from the average conditions. As a
15 second step we thus imposed more realistic temperature and wind variations on the average
16 SMR fields and used these varying fields as input for the model. Considering the uncertainties
17 of the temperature and wind fields at these altitudes the clouds produced in this way agree
18 reasonably well with OSIRIS observations. Hence, our study suggests that the temperature and
19 wind variations in the summer mesopause region are what drive the formation of the NLC, and
20 that the average fields are not enough to quantitatively describe the process of NLC
21 development. For future model studies we thus recommend to ensure that not only the averages
22 of the atmospheric fields used to drive the model, but also the variations of these fields, are in
23 agreement with observations.

Deleted: infer

Deleted: The

Deleted: At the same time it is encouraging that a microphysical model, given realistic varying temperature and wind fields, is capable of producing clouds that, in all by satellite observable aspects, agree well with the real clouds.

24 It should be pointed out that there is a clear difference in the size distribution between the clouds
25 modelled using stationary atmospheric conditions and the more realistic clouds where varying
26 temperature and wind field have been used. The former often have more Gaussian size
27 distributions whereas the latter most of the time have multimodal size distributions. Since the
28 atmosphere is non-static the assumption of a Gaussian (or any single mode) distribution should
29 be treated with care. While it may still be justified to use a single mode distribution, simply
30 from the fact that there is a limited number of free parameters one can retrieve using remote
31 sensing techniques, the user of the data should be cautious of that the ice concentrations and

Deleted: Since the latter clouds, in contrast to the former, are in good agreement with observation of the real clouds, this means that

Deleted: number densities

1 mean radii retrieved in this way are likely not in agreement with what an in-situ particle counter
2 would detect.

3 Finally, we point out that while this study has concentrated on the OSIRIS satellite retrieval
4 algorithm, the main conclusions should be similar for other satellite retrievals that are based on
5 scattering techniques and using the same assumptions for retrieving microphysical parameters.

6

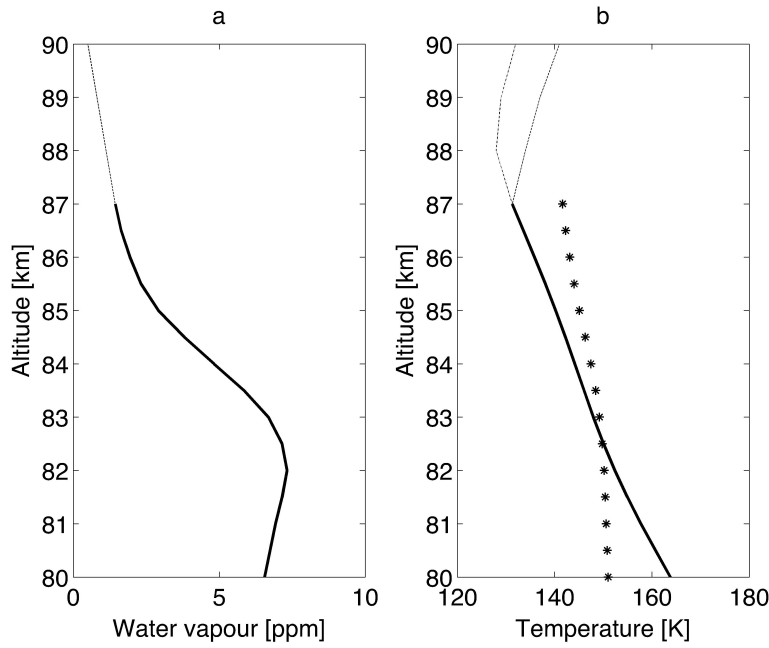
7 **Acknowledgements**

8 The authors would like to thank their colleagues, in particular the people in the particle size
9 working group, for helpful discussions. Linda Megner was supported by the Swedish
10 Research Council under contract 621-2012-1648, project 1504401. Victor I. Fomichev was
11 supported by the Canadian Space Agency.

1 **References**

Formatted: Font:Arial, Bold

2

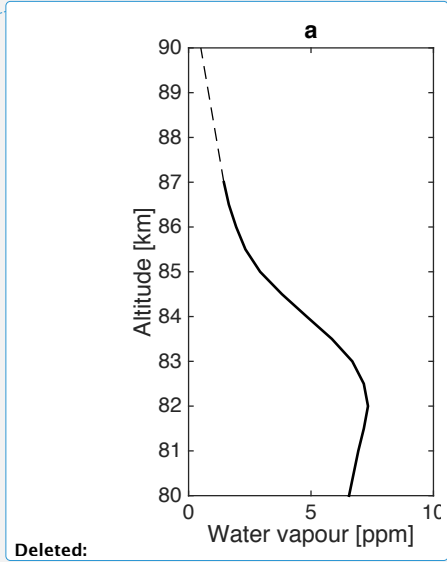


3

4 Figure 1. Input data for the “No Wave” model. (a) Average SMR water vapour (solid line) with
5 a linear extension towards higher altitudes (dashed line). (b) Average SMR temperature (solid
6 line) extended with SABER data (dashed line) and OSIRIS data (dash-dotted line). The stars
7 indicate the average frost point temperature.

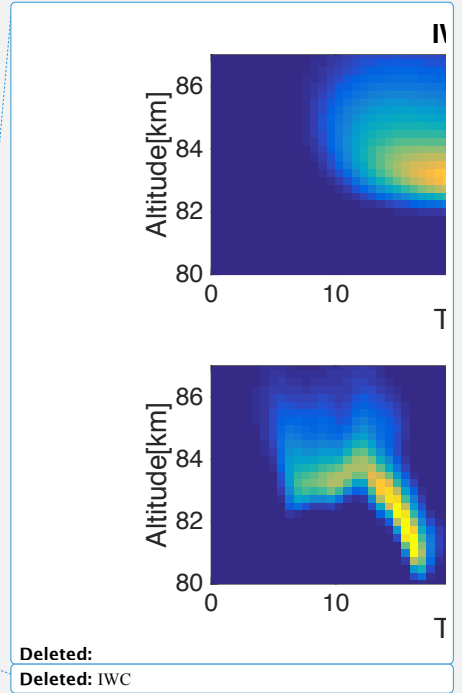
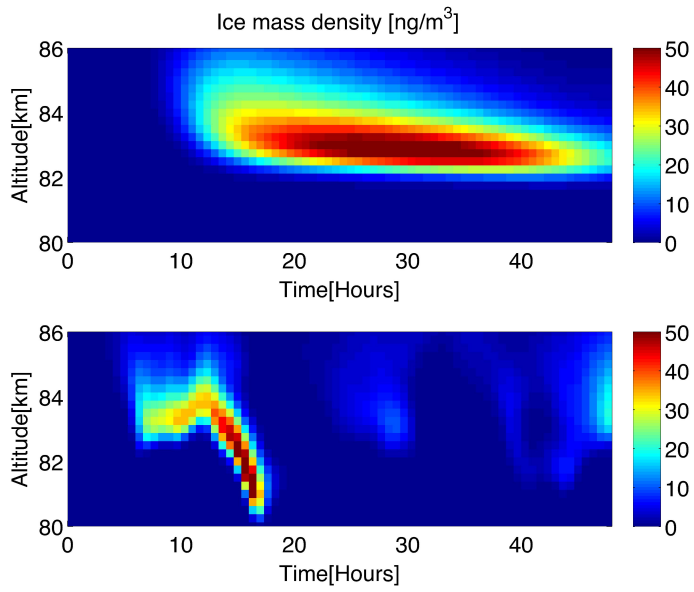
8

9



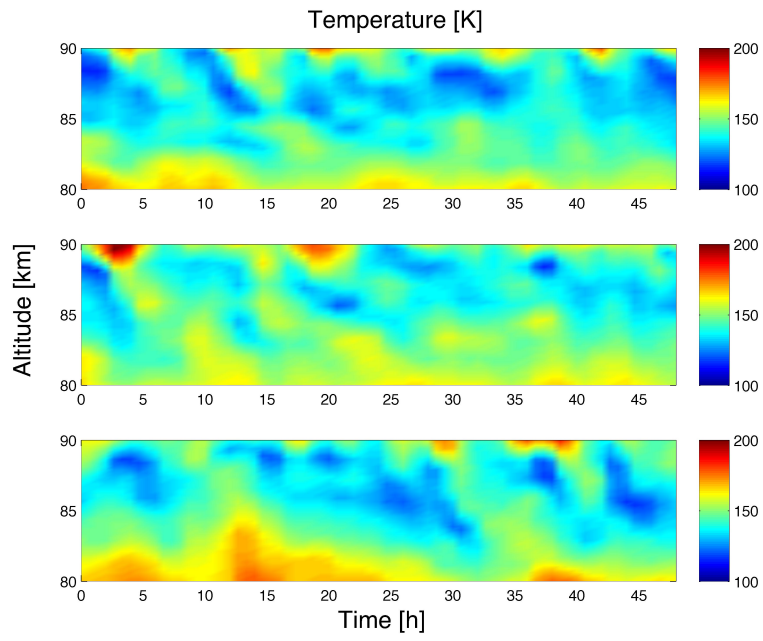
Deleted:

Deleted: OSIRIS



Deleted:
Deleted: IWC

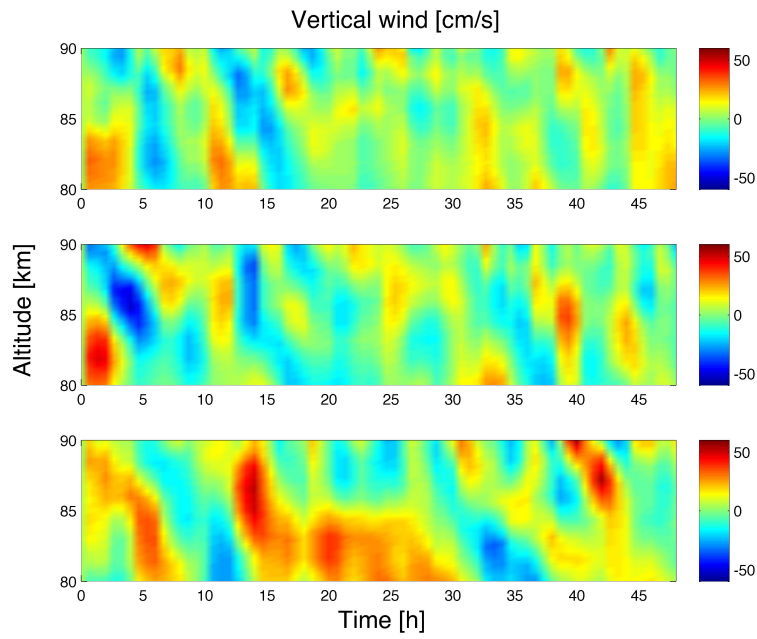
1
2 Figure 2. Ice mass density of a cloud generated by the “No Wave” model setup (top) and by the
3 “Wave” setup (bottom).
4



Deleted: [2]

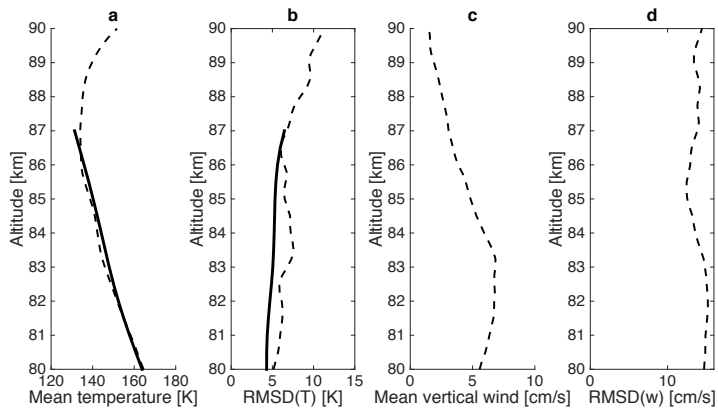
- 1
- 2 [Figure 3 Temperature fields used as input to the “Wave” model runs.](#)

Formatted: Font:12 pt, Not Bold, Font color: Accent 1, German



1

2 [Figure 4](#) Wind fields used as input to the “Wave” model runs.

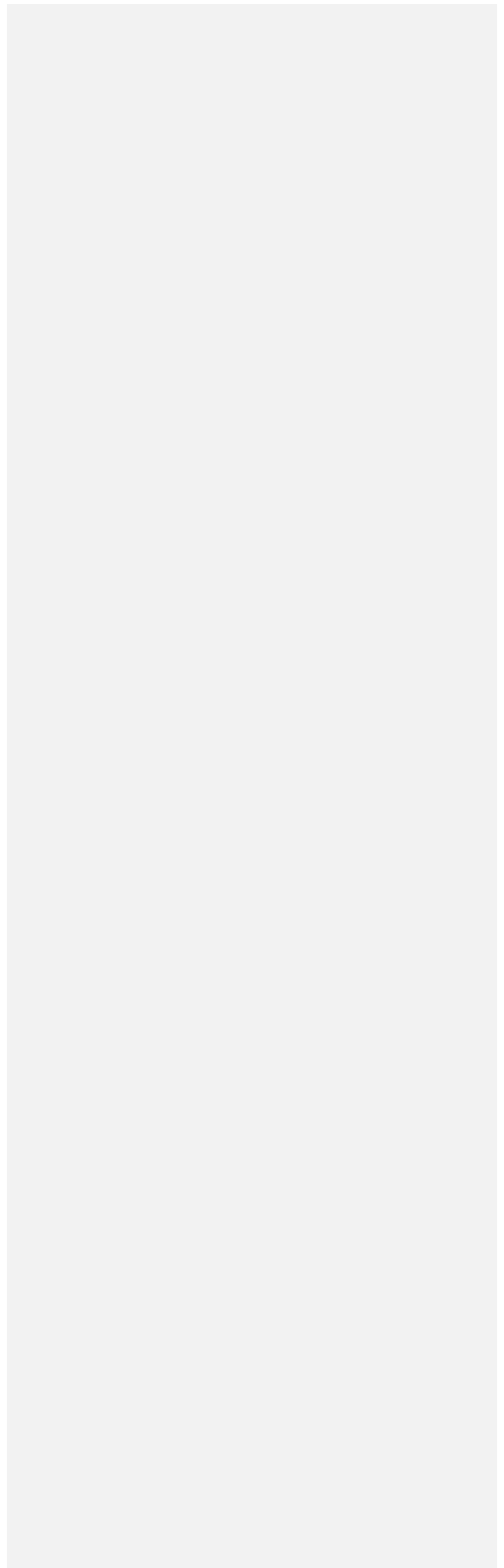


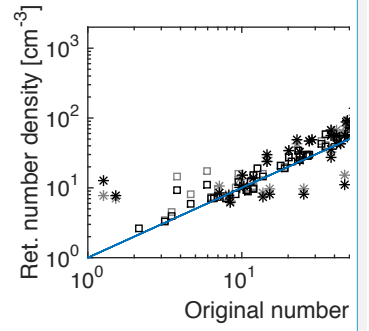
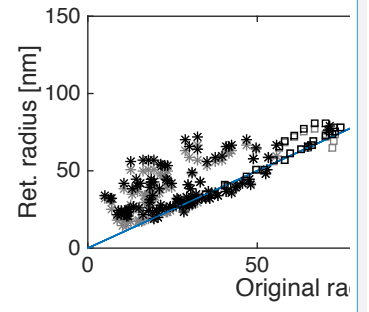
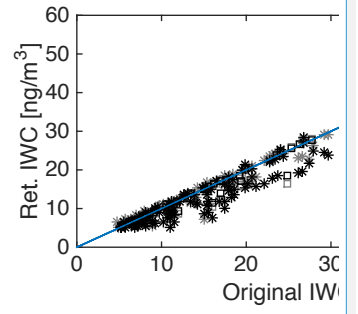
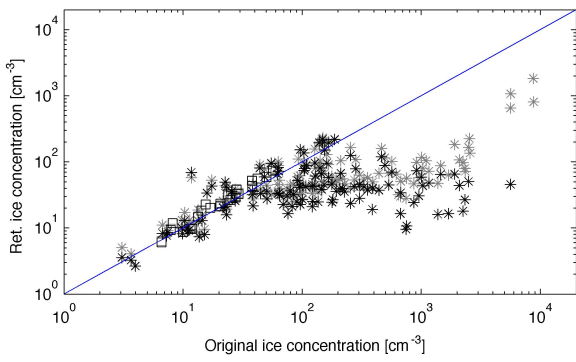
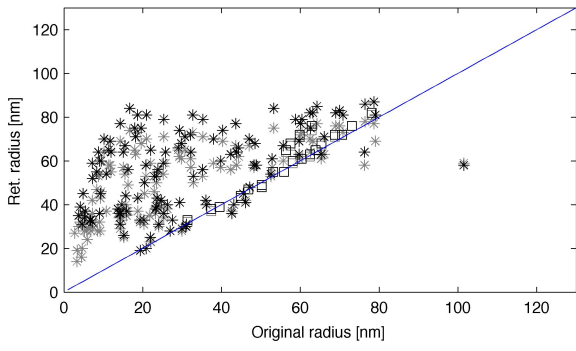
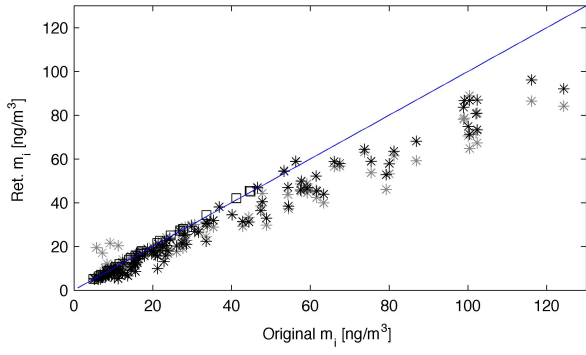
3

4 [Figure 5](#) Input to the “Wave” model setup (dashed lines). a) Adjusted average CMAM
 5 temperature and b) temperature variations. The solid lines show the same quantities for the
 6 SMR measurements. c) Average CMAM vertical winds and d) vertical wind variations.

7

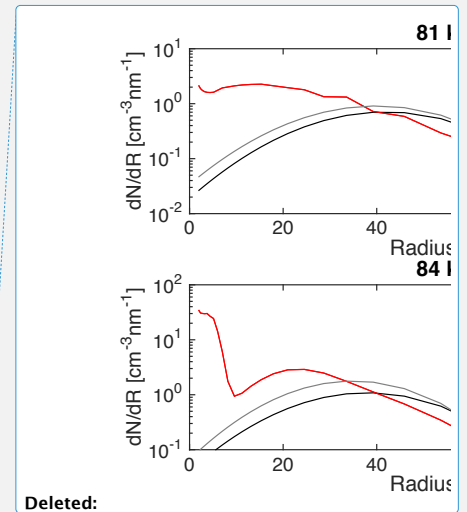
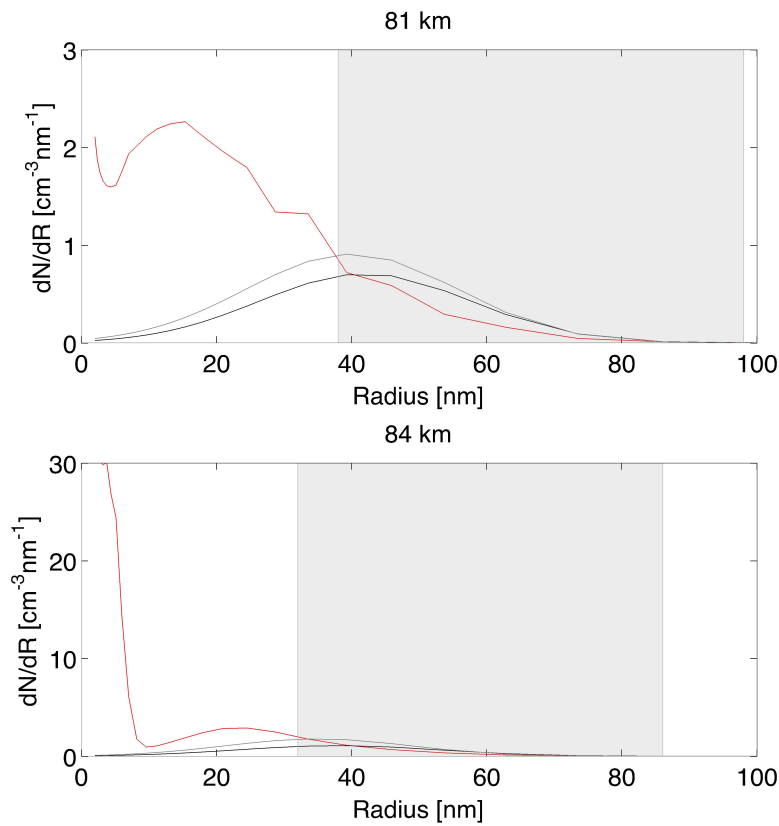
Formatted: Keep with next





Deleted:

1 Figure 6 Comparison between properties of the originally modelled clouds and what the
 2 OSIRIS retrieval algorithm calculates. Stars indicate “Wave” clouds and boxes indicate “No
 3 Wave” clouds. Black colour indicates that oblong particles with an axis ratio of 2 were assumed
 4 in the retrieval, and grey colour indicates that spherical particles were assumed.
 5

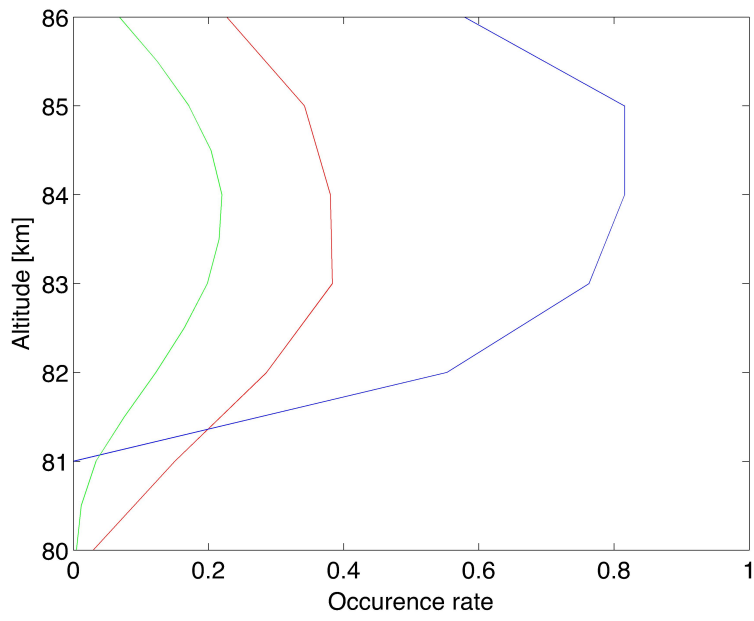


Deleted:

6
 7 Figure 7. Typical examples of size distributions of the originally modelled clouds (red) and
 8 what is retrieved by OSIRIS using an axial ratio of 2 (black) and of 1 (gray) for an altitude of
 9 81 km (top) and 84 km (bottom). [The grey area indicates the size interval where the top 90%](#)
 10 [of the total radiance comes from, to give an indication of how the large side of the particle](#)
 11 [distribution dominates the retrieval.](#)

1

2



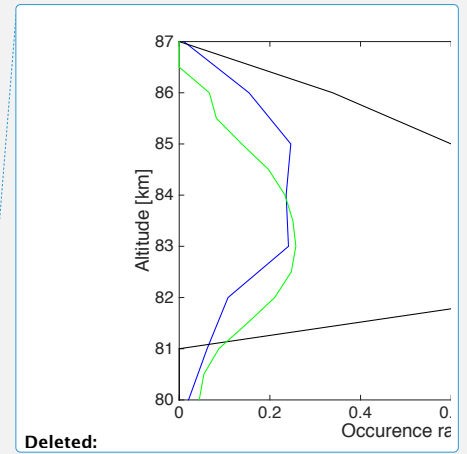
3

4 Figure 8. Frequency of occurrence for "Wave" clouds (red) and "No Wave" clouds (blue) and
 5 OSIRIS (green).

6

7

8

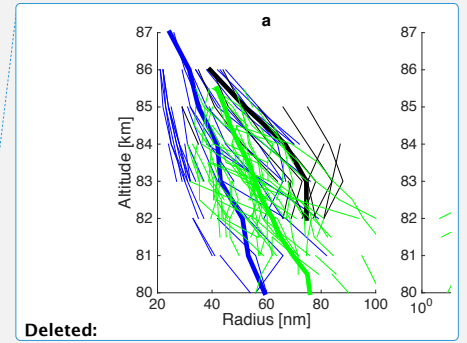
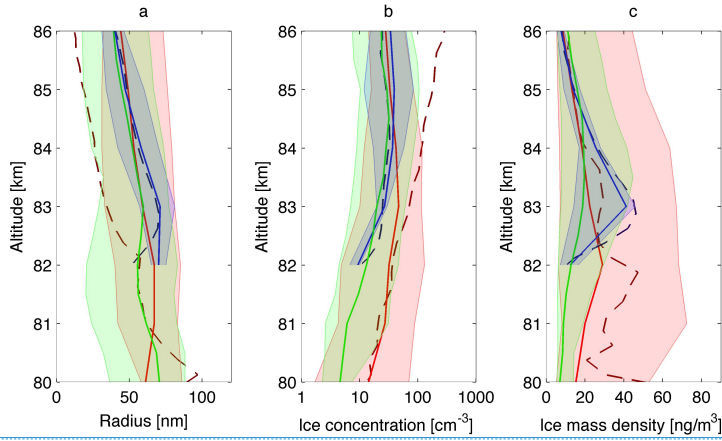


Deleted:

Deleted: blue

Deleted: black

1
2
3
4
5
6
7
8
9
10
11



- Deleted:** Mean
- Deleted:** profiles
- Deleted:** blue
- Deleted:** black
- Deleted:** modelled profiles represent snapshots of the modelled clouds with 3 h between them for "Wave" clouds and 8 h between for "No Wave" clouds. Only one out of 15 OSIRIS profiles are plotted to avoid a cluttered plot. The fat
- Deleted:** average of all profiles (not only
- Deleted:** plotted ones
- Formatted:** Keep with next
- Formatted:** Font color: Black, Swedish

1

2

3 Asmus, H., Robertson, S., Dickson, S., Friedrich, M., and Megner, L.: Charge balance for the
4 mesosphere with meteoric dust particles, *Journal of Atmospheric and Solar-Terrestrial Physics*,
5 127, 137-149, 10.1016/j.jastp.2014.07.010, 2015.

6 Bailey, Thomas, G. E., Hervig, M. E., and Lumpe, J. D.: Comparing nadir and limb
7 observations of polar mesospheric clouds: The effect of the assumed particle size distribution,
8 *Journal of Atmospheric Solar-Terrestrial Physics*, 127, 51-65, 10.1016/j.jastp.2015.02.007,
9 2015.

10 Bardeen, C. G., Toon, O. B., Jensen, E. J., Marsh, D. R., and Harvey, V. L.: Numerical
11 simulations of the three-dimensional distribution of meteoric dust in the mesosphere and upper
12 stratosphere, *Journal of Geophysical Research*, 113, 10.1029/2007JD009515, 2008.

13 Barth, C. A., Rusch, D. W., Thomas, R. J., Mount, G. H., Rottman, G. J., Thomas, G. E.,
14 Sanders, R. W., and Lawrence, G. M.: Solar Mesosphere Explorer: Scientific objectives and
15 results, *Geophysical Research Letters*, 10, 237-240, 10.1029/GL010i004p00237, 1983.

16 Baumgarten, G., Fiedler, J., and Rapp, M.: On microphysical processes of noctilucent clouds
17 (NLC): observations and modeling of mean and width of the particle size-distribution,
18 *Atmospheric Chemistry and Physics*, 10, 5194/acp-10-6661-2010, 2010.

19 Beagley, S. R., Boone, C. D., Fomichev, V. I., Jin, J. J., Semeniuk, K., McConnell, J. C., and
20 Bernath, P. F.: First multi-year occultation observations of CO₂ in the MLT by ACE satellite:
21 observations and analysis using the extended CMAM, *Atmos. Chem. Phys.*, 10, 1133-1153,
22 10.5194/acp-10-1133-2010, 2010.

23 Berger, U.: Icy particles in the summer mesopause region: Three-dimensional modeling of their
24 environment and two-dimensional modeling of their transport, *Journal of Geophysical*
25 *Research*, 107, 10.1029/2001JA000316, 2002.

26 Chandran, A., Rusch, D. W., Thomas, G. E., Palo, S. E., Baumgarten, G., Jensen, E. J., and
27 Merkel, A. W.: Atmospheric gravity wave effects on polar mesospheric clouds: A comparison
28 of numerical simulations from CARMA 2D with AIM observations, *Journal of Geophysical*
29 *Research: Atmospheres*, 117, 10.1029/2012JD017794, 2012.

30 Christensen, O. M., Eriksson, P., Urban, J., Murtagh, D., Hultgren, K., and Gumbel, J.:
31 Tomographic retrieval of water vapour and temperature around polar mesospheric clouds using
32 Odin-SMR, *Atmospheric Measurement Techniques*, 8, 1981-1999, 2015.

33 Colella, P., and Woodward, P. R.: The Piecewise Parabolic Method (PPM) for gas-dynamical
34 simulations, *Journal of Computational Physics*, 54, 174-201, [http://dx.doi.org/10.1016/0021-](http://dx.doi.org/10.1016/0021-9991(84)90143-8)
35 [9991\(84\)90143-8](http://dx.doi.org/10.1016/0021-9991(84)90143-8), 1984.

36 [Eremenko, M. N., Petelina, S. V., Zsetsky, A. Y., Karlsson, B., Rinsland, C. P., Llewellyn, E.](#)
37 [J. and Sloan, J. J.: Shape and composition of PMC particles derived from satellite remote](#)
38 [sensing measurements, *Geophysical Research Letters*, 32, L16S06, 10.1029/2005GL023013,](#)
39 [2005](#)

40 Fletcher, N. H.: Size Effect in Heterogeneous Nucleation, *The Journal of Chemical Physics*, 29,
41 572-576, doi:<http://dx.doi.org/10.1063/1.1744540>, 1958.

1 Fomichev, V. I., Ward, W. E., Beagley, S. R., McLandress, C., McConnell, J. C., McFarlane,
2 N. A., and Shepherd, T. G.: Extended Canadian Middle Atmosphere Model: Zonal-mean
3 climatology and physical parameterizations, *Journal of Geophysical Research*, 107, 4087,
4 10.1029/2001JD000479, 2002.

5 Gumbel, J., and Megner, L.: Charged meteoric smoke as ice nuclei in the mesosphere: Part 1—
6 A review of basic concepts, *Journal of Atmospheric and Solar-Terrestrial Physics*, 71, 1225-
7 1235, <http://dx.doi.org/10.1016/j.jastp.2009.04.012>, 2009.

8 Hansen, G., Serwazi, M., and von Zahn, U.: First detection of a noctilucent cloud by lidar,
9 *Geophysical Research Letters*, 16, 1445-1448, 10.1029/GL016i012p01445, 1989.

10 Hedin, J., Gumbel, J., and Rapp, M.: On the efficiency of rocket-borne particle detection in the
11 mesosphere, *Atmos. Chem. Phys.*, 7, 3701-3711, 10.5194/acp-7-3701-2007, 2007.

12 Höffner, J., and Lübken, F. J.: Potassium lidar temperatures and densities in the mesopause
13 region at Spitsbergen (78°N), *Journal of Geophysical Research: Atmospheres* (1984–2012),
14 112, 10.1029/2007jd008612, 2007.

15 Hultgren, K., Gumbel, J., Degenstein, D., Bourassa, A., Lloyd, N., and Stegman, J.: First
16 simultaneous retrievals of horizontal and vertical structures of [polar mesospheric clouds](#) from
17 Odin/OSIRIS tomography, *Journal of Atmospheric and Solar-Terrestrial Physics*, 104, 213-
18 223, 2013.

19 Hultgren, K., and Gumbel, J.: Tomographic and spectral views on the lifecycle of polar
20 mesospheric clouds from Odin/OSIRIS, *Journal of Geophysical Research: Atmospheres*, 119,
21 10.1002/2014jd022435, 2014.

22 Hunten, D.M., Turco, R.P. and Toon, O.B.: Smoke and dust particles of meteoric origin in the
23 Mesosphere and Stratosphere, *Journal of the Atmospheric Sciences*, 37, 1342-1357, 1980

24 Karlsson, B., and Gumbel, J.: Challenges in the limb retrieval of noctilucent cloud properties
25 from Odin/OSIRIS, *Advances in Space Research*, 36, 935-942,
26 <http://dx.doi.org/10.1016/j.asr.2005.04.074>, 2005.

27 Keesee, R. G.: Nucleation and particle formation in the upper atmosphere, *Journal of*
28 *Geophysical Research: Atmospheres*, 94, 14683-14692, 10.1029/JD094iD12p14683, 1989.

29 [Kiliani, J., Baumgarten, G., Lübken, F.-J., and Berger, U.: Impact of particle shape on the](#)
30 [morphology of noctilucent clouds, *Atmos. Chem. Phys.*, 15, 12897-12907, 10.5194/acp-15-](#)
31 [12897-2015, 2015.](#)

32 Leslie, R.: Sky glows, *Nature*, 32, 245, 1885.

33 Llewellyn, E. J., Lloyd, N. D., Degenstein, D. A., Gattinger, R. L., Petelina, S., and Bourassa,
34 A. E.: The OSIRIS instrument on the Odin spacecraft, *Canadian Journal of Physics*, 82, 411-
35 422, 10.1139/p04-005, 2004.

36 Lübken, F.-J., Rapp, M., and Strelnikova, I.: The sensitivity of mesospheric ice layers to
37 atmospheric background temperatures and water vapor, *Advances in Space Research*, 40, 794-
38 801, <http://dx.doi.org/10.1016/j.asr.2007.01.014>, 2007.

39 Lübken, F. J.: Seasonal variation of turbulent energy dissipation rates at high latitudes as
40 determined by in situ measurements of neutral density fluctuations, *Journal of Geophysical*
41 *Research: Atmospheres*, 102, 13441-13456, 10.1029/97JD00853, 1997.

42 McLandress, C., Ward, W. E., Fomichev, V. I., Semeniuk, K., Beagley, S. R., McFarlane, N.
43 A., and Shepherd, T. G.: Large-scale dynamics of the mesosphere and lower thermosphere: An

Deleted: Polar Mesospheric Clouds

1 analysis using the extended Canadian Middle Atmosphere Model, *Journal of Geophysical*
2 *Research*, 111, 10.1029/2005JD006776, 2006.

3 Megner, L., Rapp, M., and Gumbel, J.: Distribution of meteoric smoke–sensitivity to
4 microphysical properties and atmospheric conditions, *Atmospheric Chemistry and Physics*, 6,
5 4415-4426, 10.5194/acp-6-4415-2006, 2006.

6 Megner, L., Gumbel, J., Rapp, M., and Siskind, D. E.: Reduced meteoric smoke particle density
7 at the summer pole – Implications for mesospheric ice particle nucleation, *Advances in Space*
8 *Research*, 41, 10.1016/j.asr.2007.09.006, 2008a.

9 Megner, L., Siskind, D. E., Rapp, M., and Gumbel, J.: Global and temporal distribution of
10 meteoric smoke: A two-dimensional simulation study, *Journal of Geophysical Research:*
11 *Atmospheres* 113, 10.1029/2007JD009054, 2008b.

12 Megner, L., and Gumbel, J.: Charged meteoric particles as ice nuclei in the mesosphere: Part 2,
13 *Journal of Atmospheric and Solar-Terrestrial Physics*, 71, 10.1016/j.jastp.2009.05.002, 2009.

14 Megner, L.: Minimal impact of condensation nuclei characteristics on observable Mesospheric
15 ice properties, *Journal of Atmospheric and Solar-Terrestrial Physics*, 73,
16 10.1016/j.jastp.2010.08.006, 2011.

17 Merkel, A. W., Marsh, D. R., Gettelman, A., and Jensen, E. J.: On the relationship of polar
18 mesospheric cloud ice water content, particle radius and mesospheric temperature and its use
19 in multi-dimensional models, *Atmos. Chem. Phys.*, 9, 8889-8901, 10.5194/acp-9-8889-2009,
20 2009.

21 Nordh, H. L., Schéele, F. v., Frisk, U., Ahola, K., Booth, R. S., Encrenaz, P. J., Hjalmarson, Å.,
22 Kendall, D., Kyrölä, E., Kwok, S., Lecacheux, A., Leppelmeier, G., Llewellyn, E. J., Mattila,
23 K., Mégie, G., Murtagh, D., Rougeron, M., and Witt, G.: The Odin orbital observatory, *A&A*,
24 402, L21-L25, 2003.

25 Rapp, M., and Thomas, G. E.: Modeling the microphysics of mesospheric ice particles:
26 Assessment of current capabilities and basic sensitivities, *Journal of Atmospheric and Solar-*
27 *Terrestrial Physics*, 68, 10.1016/j.jastp.2005.10.015, 2006.

28 Roddy, A. F.: The role of meteoric particles in noctilucent clouds, *Irish Astronomical Journal*,
29 16, 194-202, 1984.

30 Sheese, P. E., Llewellyn, E. J., Gattinger, R. L., Bourassa, A. E., Degenstein, D. A., Lloyd, N.
31 D., and McDade, I. C.: Mesopause temperatures during the polar mesospheric cloud season,
32 *Geophysical Research Letters*, 38, 10.1029/2011GL047437, 2011.

33 Stevens, M. H.: The polar mesospheric cloud mass in the Arctic summer, *Journal of*
34 *Geophysical Research*, 110, 10.1029/2004JA010566, 2005.

35 Toon, O. B., Turco, R. P., Hamill, P., Kiang, C. S., and Whitten, R. C.: A One-Dimensional
36 Model Describing Aerosol Formation and Evolution in the Stratosphere: II. Sensitivity Studies
37 and Comparison with Observations, *Journal of the Atmospheric Sciences*, 36, 718-736,
38 10.1175/1520-0469(1979)036<0718:AODMDA>2.0.CO;2, 1979.

39 Turco, R. P., Hamill, P., Toon, O. B., Whitten, R. C., and Kiang, C. S.: A One-Dimensional
40 Model Describing Aerosol Formation and Evolution in the Stratosphere: I. Physical Processes
41 and Mathematical Analogs, *Journal of the Atmospheric Sciences*, 36, 699-717, 10.1175/1520-
42 0469(1979)036<0699:AODMDA>2.0.CO;2, 1979.

- 1 Turco, R. P., Toon, O. B., Whitten, R. C., Keesee, R. G., and Hollenbach, D.: [noctilucent](#)
2 clouds: Simulation studies of their genesis, properties and global influences, Planetary and
3 Space Science, 30, 1147-1181, 1982.
- 4 Vergados, P., and Shepherd, M. G.: Retrieving mesospheric water vapour from observations of
5 volume scattering radiances, Annales Geophysicae, 27, 487-501, 10.5194/angeo-27-487-2009,
6 2009.
- 7 [von Savigny, C., Petelina, S.V., Karlsson, B., et al. Vertical variation of NLC particle sizes](#)
8 [retrieved from Odin/OSIRIS limb scattering observations. Geophysical Research Letters, 32,](#)
9 [L07806, 10.1029/2004GL02198, 2005](#)
- 10 Witt, G.: Polarization of light from noctilucent clouds, Journal of Geophysical Research, 65,
11 925-933, 10.1029/JZ065i003p00925, 1960.
- 12

Deleted: Noctilucent

Another aspect where there is better agreement between the OSIRIS observations and the “Wave” clouds as compared to the “No Wave” clouds is where in the cloud layer the different quantities peak. For the OSIRIS observations and the “Wave” clouds the number density generally increases with altitude peaking above the IWC, whereas the mean radii increases with decreasing altitude and peaks at the bottom of the clouds, i.e. lower than the maximum IWC. For the “No Wave” clouds the individual profiles for mean radii, number density and IWC tend to peak at the same altitude (in Figure 7a we can see that some of the individual profiles show smaller mean radii at 83 km than at 82 km but these are the data points that were subject to retrieval issues as discussed in Section 4.3 and showed by the squares below the line in Figure 4b).

To summarize it is clear that the “Wave” clouds agree well with the observations, whereas the “No Wave” clouds, despite having been tuned to the correct IWC, show different characteristics.

